Supplementary Information: Activity-based contact network scaling and epidemic propagation in metropolitan areas

Nishant Kumar[1], Jimi B. Oke[2], and Bat-hen Nahmias-Biran[3]

[1]Future Resilient Systems, Singapore-ETH Centre, Singapore- 138602
[2]Department of Civil and Environmental Engineering, University of Massachusetts, Amherst, MA 01003, United States
[3]Department of Civil Engineering, Ariel University, Ariel 40700, Israel

June 10, 2020

1 Age dependent transition probabilites for the modified SEIRD model

For ease of reference, we briefly represent the model and the variables representing the probability of transition between various states.

- $\boldsymbol{S}$: susceptible
- $\boldsymbol{E}$: exposed (infected, not contagious)
- $\boldsymbol{I}^S$: infectious, symptomatic (clinical)
- $\boldsymbol{I}^A$: infectious, asymptomatic (subclinical)
- $\boldsymbol{R}$: recovered
- $\boldsymbol{D}$: deceased

The transitions to each of these states are governed by the probabilities as shown in Figure 1. In this section, we limit our discussion to ρ and μ since these two variables have been reported as highly age-dependent [1]. All the other transition variables (*viz.* ϕ, κ and γ) are modeled as being independent of the age of the agent.

We refer to Table 1 and obtain the agent-specific value of ρ using the agent's age. Prior to starting the simulation, we use this value of ρ to mark the agents for their transition to I^A or I^S. This implies, should an agent become infected (E) during the course of the simulation, his transition to I^A or I^S is predetermined.

Given that case fatality rate (CFR) has been shown to differ significantly by age group, we use the values estimated by [2], who provide adjusted posterior mode estimates of the CFR, given measuremenst over 41 days, along with 95% credible intervals. We assume the CFR is obtained from

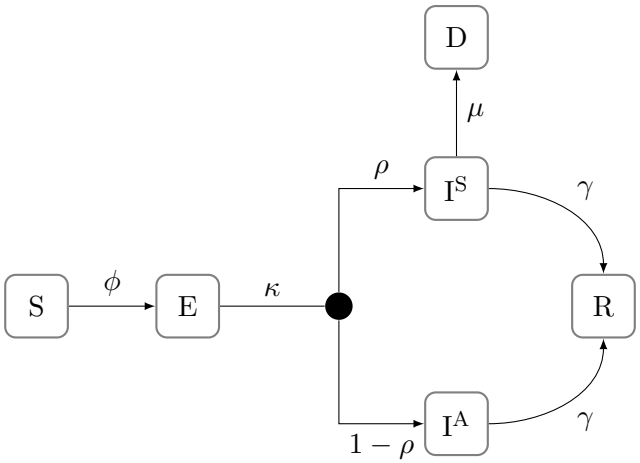

Supplementary Figure 1 Susceptible-Exposed-Infectious-Recovered-Deceased epidemiological model framework. ϕ is the transmission probability, while κ is the probability of transitioning from an exposed state to an infectious one. ρ is the age-dependent probability that an infectious individual will be symptomatic. μ is probability that an infectious individual will be deceased, while γ is the probability of recovery.

Age	$\boldsymbol{\rho}$
0-9	0.4
10-19	0.4
20-29	0.8
30-39	0.8
40-49	0.8
50-59	0.8
60-69	0.8
70-79	0.8
$\geq$80	0.8

Supplementary Table 1 Age related values of the probability of symptomatic infectiousness, ρ, obtained from [1] based on measurements taken in China. With more granular data, these can be updated for greater detail in simulating the epidemic across various age groups.

the CDF of an underlying exponential distribution governing the duration from onset of COVID-19 to death. Thus:

$$P(T > 41) = CFR \tag{1}$$

$$1 - e^{-41/d_D} = CFR \tag{2}$$

$$\implies \hat{d}_D = -\frac{t}{\ln(1 - CFR)} \tag{3}$$

The value of d_D computed from the above equation is taken as the median of the lognormal random variate. Thus, the mean of the associated normal distribution is obtained by $\mu_{\ln d_D} = \ln(\hat{d}_D)$. We also compute the variance of d_D using the sample sizes and credible intervals computed by [2] to compute upper and lower bounds for d_D. Finally, we estimate the variance of the associated normal distribution, that is $\sigma^2_{\ln d_D}$ by solving the transcendental equations relating the parameters

of the lognormal distribution to those of the associated normal distribution. A summary of the parameters are shown in Table 2.

Age	**Sample Size**	**CFR (95% CI)**	$\hat{\mu}_{\ln d_D}$ **(95% CI)**	$\hat{\sigma}_{d_D}$	$\hat{\sigma}_{\ln d_D}$
0–9	$4.160 \cdot 10^2$	$2.600 \cdot 10^{-5}$ ($3.120 \cdot 10^{-6}$, $3.820 \cdot 10^{-4}$)	$6.782 \cdot 10^7$ ($1.314 \cdot 10^7$, $1.073 \cdot 10^5$)	$1.427 \cdot 10^1$	1.942
10–19	$5.490 \cdot 10^2$	$1.400 \cdot 10^{-4}$ ($2.880 \cdot 10^{-5}$, $7.590 \cdot 10^{-4}$)	$8.186 \cdot 10^6$ ($1.424 \cdot 10^6$, $5.400 \cdot 10^4$)	$1.259 \cdot 10^1$	1.830
20–29	$3.619 \cdot 10^3$	$6.000 \cdot 10^{-4}$ ($3.170 \cdot 10^{-4}$, $1.320 \cdot 10^{-3}$)	$1.508 \cdot 10^6$ ($1.293 \cdot 10^5$, $3.104 \cdot 10^4$)	$1.113 \cdot 10^1$	1.765
30–39	$7.600 \cdot 10^3$	$1.460 \cdot 10^{-3}$ ($1.030 \cdot 10^{-3}$, $2.550 \cdot 10^{-3}$)	$5.277 \cdot 10^5$ ($3.979 \cdot 10^4$, $1.606 \cdot 10^4$)	$1.024 \cdot 10^1$	1.720
40–49	$8.571 \cdot 10^3$	$2.950 \cdot 10^{-3}$ ($2.210 \cdot 10^{-3}$, $4.220 \cdot 10^{-3}$)	$2.087 \cdot 10^5$ ($1.853 \cdot 10^4$, $9.695 \cdot 10^3$)	9.538	1.656
50–59	$1.001 \cdot 10^4$	$1.250 \cdot 10^{-2}$ ($1.030 \cdot 10^{-2}$, $1.550 \cdot 10^{-2}$)	$3.408 \cdot 10^4$ ($3.960 \cdot 10^3$, $2.625 \cdot 10^3$)	8.089	1.548
60–69	$8.583 \cdot 10^3$	$3.990 \cdot 10^{-2}$ ($3.410 \cdot 10^{-2}$, $4.550 \cdot 10^{-2}$)	$7.121 \cdot 10^3$ ($1.182 \cdot 10^3$, $8.804 \cdot 10^2$)	6.915	1.423
70–79	$3.918 \cdot 10^3$	$8.610 \cdot 10^{-2}$ ($7.480 \cdot 10^{-2}$, $9.990 \cdot 10^{-2}$)	$2.201 \cdot 10^3$ ($5.274 \cdot 10^2$, $3.896 \cdot 10^2$)	6.121	1.296
≥ 80	$1.408 \cdot 10^3$	$1.340 \cdot 10^{-1}$ ($1.120 \cdot 10^{-1}$, $1.590 \cdot 10^{-1}$)	$1.038 \cdot 10^3$ ($3.452 \cdot 10^2$, $2.368 \cdot 10^2$)	5.652	1.195

Supplementary Table 2 Age-dependent case fatality rate (CFR) parameters. The number of days from onset to death d_D is assumed to be lognormally distributed. The CFR (95% CI) and sample size for respective age categories are obtained from [2]. The reported CFR values are taken as the CDF of an exponential distribution with mean rate of occurrence $\frac{1}{d_D}$ at day 41. The computed d_D is then taken as the median of the associated lognormal distribution, from which the parameters of the associated normal distribution, $\hat{\mu}_{\ln d_D}$ and $\hat{\sigma}_{\ln d_D}$, are computed.

2 Modeling contact intensity

To properly model the contact intensity, we need to estimate the mean distance between agents (persons) at each node or vehicle. For any location where interaction might occur, we model the distances between agents by assigning them random locations within the area. The vehicles and nodes are treated differently.

2.1 Distances between agents in vehicles

In the case of public transit vehicles, the shape of vehicle is always a rectangle. However, we assume the exposure to be limited to the immediate square a passenger is in. Hence, we assume the area of potential exposure to be a square of size equal to the width of the vehicle. Motivated by the data on average dimensions of vehicles, we make the following assumptions for the effective area of exposure within the vehicles:

$$A_{\text{train}} = \frac{1}{5} * \text{ [average area of train } \textit{car}\text{]} \tag{4}$$

$$A_{\text{bus}} = \frac{1}{4} * \text{[average area of a bus]} \tag{5}$$

$$A_{\text{PV}} = \text{average area of a car} \tag{6}$$

Based on the assumptions made above, the effective number of infectious people to which an agent can be exposed to is also limited to the relevant sample of total number of infectious agents on the vehicle. If total number of infectious agents on a vehicle at any given time is given by

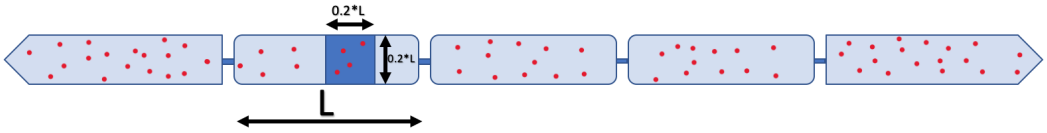

(A)

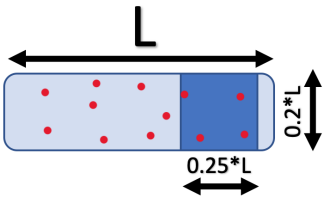

(B)

SUPPLEMENTARY FIGURE 2 Illustration showing assumptions for potential exposure areas in case of Figure 2a: train and Figure 2b: Bus

$N_I[vehicle]$, the effective number($N_{EI}[vehicle]$) of infectious people can be summarised as follows:

$$N_{EI}[train] = \frac{1}{5} * \frac{1}{5} * N_I[train]; \text{assuming 5 cars in a train} \tag{7}$$

$$N_{EI}[bus] = \frac{1}{4} * N_I[bus] \tag{8}$$

$$N_{EI}[PV] = N_I[car] \tag{9}$$

$$\tag{10}$$

To each agent, we assign a random location chosen uniformly within the potential area of exposure. An illustration showing the potential exposure areas for train and buses is shown in Figure 2. This is followed by computing the Euclidean distance between the agents based on these uniformly assigned locations. For faster implementation purposes, we use the mean of Euclidean distances instead. The use of mean distances is justified because the mean Euclidean distance between two agents converges to the expected distance very fast with increasing number of agents as shown in Figure 3. (See [3] for a detailed treatment of these results).

2.2 Distances between agents performing activity at a node

We partition the area of the cities into representative areas for each node of the transportation network. We use Voronoi tessellations with a clipping threshold to represent a realistic partition. The clipping threshold is selected such that post clipping, the sum of all areas, is equal to the area of the respective metros. Post clipping, a visual representation of the node-specific representative areas for both cities are shown in Figure 6.

For ease of representation, we convert these node areas to circular regions of equal as shown in Figure 5a. Given the number of infectious agents at the respective node (N_I), we choose N_I points on the circle using a Gaussian centered at the centre of the circle. The variance of the Gaussian is proportional to the area of the circle. The proportion is chosen such that 95% of the points fall within the area of the circle (Figure 5b). Using this relation between variance and area, we capture the idea that the agents are distributed throughout the representative area of the node.

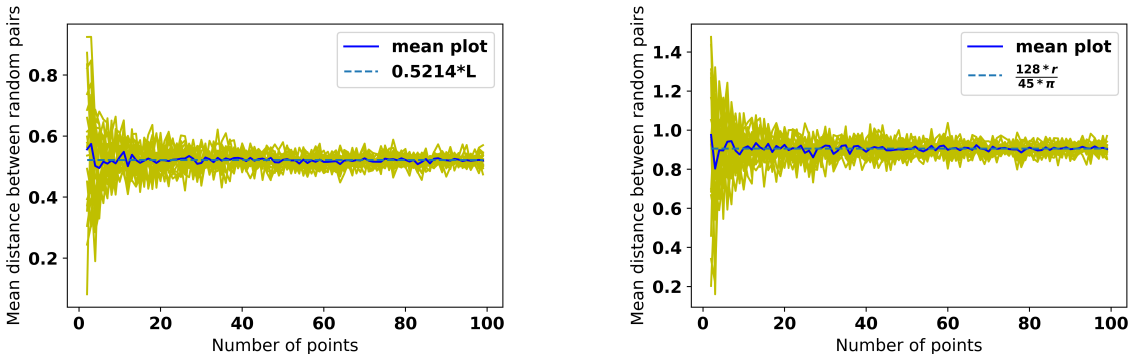

(A) Mean distance for unit square

(B) Mean distance for unit circle

SUPPLEMENTARY FIGURE 3 Fast convergence of mean distance with number of points (N)

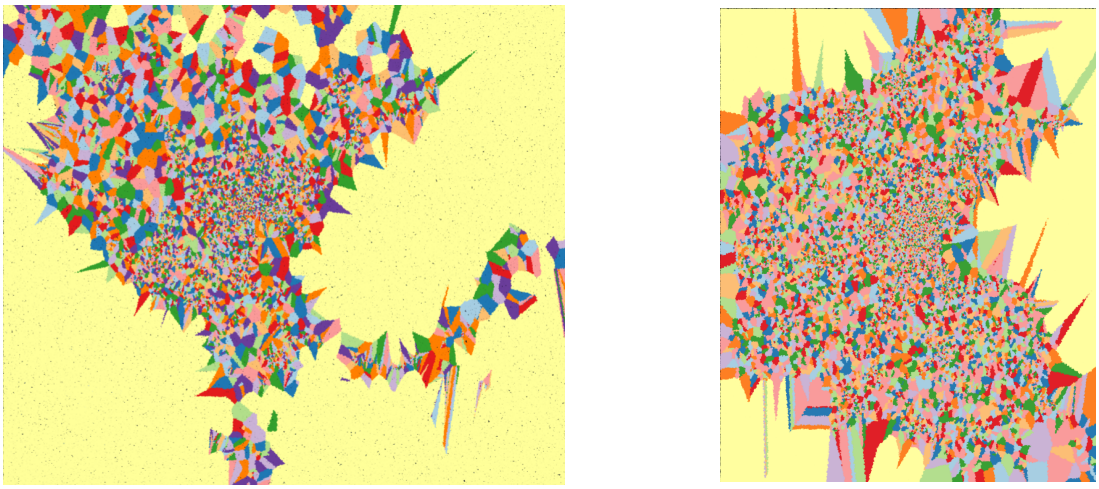

(A) *Auto Sprawl*

(B) *Auto Innovative*

SUPPLEMENTARY FIGURE 4 Representative areas of nodes for each city

The Gaussian nature of location assignment captures the idea that hot-spot areas of the node have a higher density of agents at any given time.

2.2.1 Distances between agents staying at home

The treatment of home is similar to a square vehicle of area 223 m^2, as given by the survey from US census bureau [4].

3 Contact network

A contact network carries information about the frequency and intensity of contacts between the agents at different points in space and time. We accomplish the creation of the contact network from the output of transportation simulation by separate treatment of different modes of the interaction within the network. The interaction can be either in a stationary location (e.g. a node of the city) or while traveling. Each type of interaction is a contact network. We create separate contact graphs for the three most relevant types of interactions: interactions while using public transit,

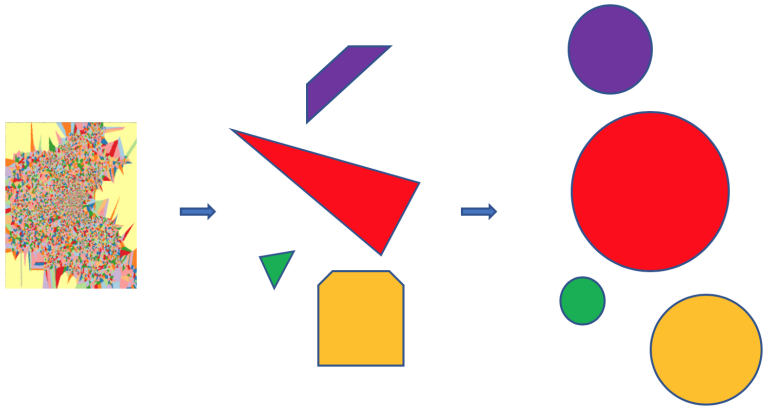

(A) Circular representations of Voronoi areas shown for three sample nodes

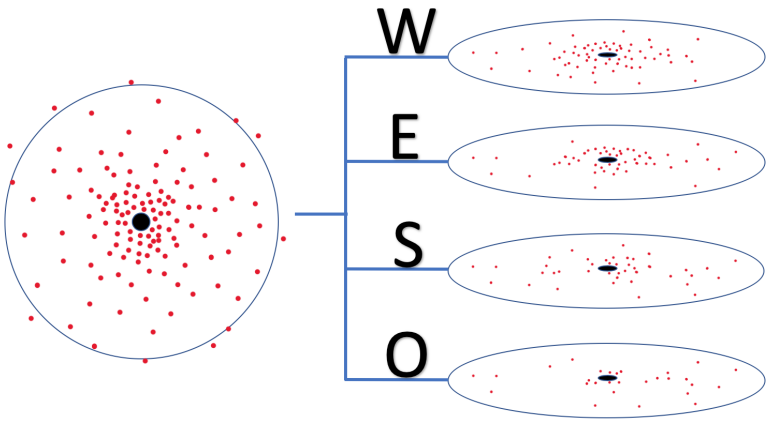

(B) Splitting of agent into layers according to activity (W: *Work*, E: *Education*, S: *Shopping*, O: *Other*)

SUPPLEMENTARY FIGURE 5 Assigning random locations to agents at a node

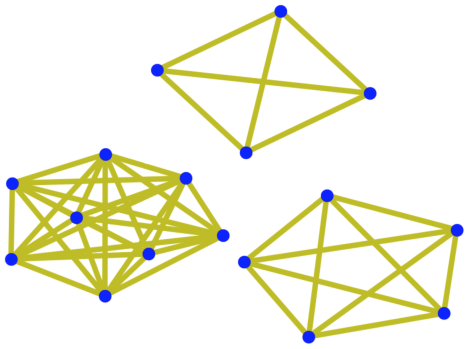

(A) $G[t]$: Contact graph at time t

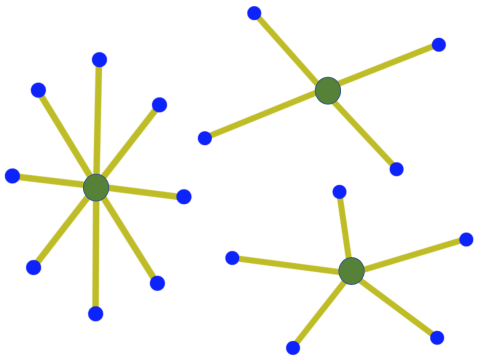

(B) Hub and spoke representation of $G[t]$. Each green vertex is a dummy vertex introduced to represent a location of potential contact. (viz. a bus, train, home or a node of city)

SUPPLEMENTARY FIGURE 6 Two representations of the contact graph. The blue vertices represent agents while green vertices represent a location. The edges are not weighted in this representation and are not linked to the intensity of contact between agents.

interactions while performing an activity at a node of the city and interactions while staying at home. A union of these individual contact graphs gives us the full contact network for the city. We assume that the individuals who choose to drive alone, do not come into contact with anyone else during the course of the journey. Hence, we do not account for driving as an activity.

3.1 Temporal split

In order to simplify the construction of the contact network, we split the contact network into networks at different times of the day. The temporal resolution of contact network used in our simulations is 5 minutes. The contact network at any 5 minute window is a graph with several disconnected components, each component being a clique as shown in Figure 6a. Each clique represents a location where interaction between agents might occur. At any given time all the agents present at a given location represent the nodes of the clique.

The size of each clique is equal to the number of agents at the corresponding location. In order to handle large number of agents, we simplify the graph structure and transform each clique to a hub-and-spoke structure as shown in Figure 6b. This transformation significantly reduces the number of edges in the graph and as a consequence, reduces the computing resources required to carry out the simulation. The hub-and-spoke representation is conveniently represented using the data structure discussed in Section 6

3.2 Spatial split for activities

The construction of the contact network ensures that different locations in space are represented as a standalone component. However, the activities contact network is an exception to this. In case of the activities network, several agents present at the same node of the city may be performing a different class of activity, hence do not run a risk of interaction. In order to model this, we split the activity contact network at a node into different layers based on the type of activity as shown in Figure 5b. Thus, only intra-layer interactions between agents are allowed.

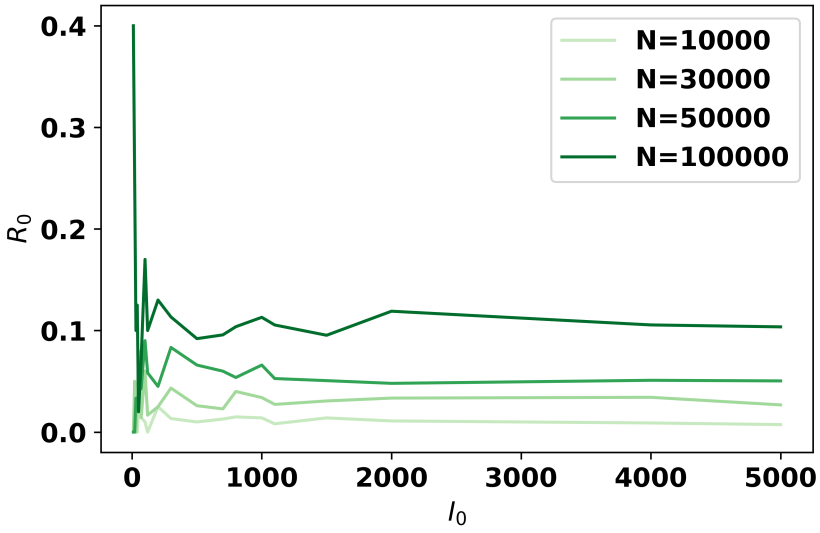

SUPPLEMENTARY FIGURE 7 Basic reproductive number R_0 versus the initial number of infected agents I_0 for a fixed values of Θ'. In order to study this behavior of R_0, we sampled three different sized sets of individuals from *Auto Sprawl* and set a small Θ'. The I_0 was chosen between 0 and 5000 with more samples for smaller values.

4 Calibration

To find Θ, we calibrate in order to achieve a basic reproductive number (average number of secondary cases caused by an infected person in the early stage of the epidemic) of $R_0 = 2.5$ using:

$$R_0 = \frac{1}{X} \sum_{m}^{X} \sum_{n}^{S} \left(1 - e^{-\Theta' \sum_m \tau_{nm}}\right) \tag{11}$$

where $\Theta' = \Theta q_0, i_0$. We use the above equation to solve for Θ'.

We notice that if we calibrate Θ' for an $R_0 = 2.5$ for a contact network generated using a sample of the population, the same Θ' does not provide a resultant $R_0 = 2.5$ when simulating with the full population. It results in very high values of R_0. We hypothesize that this behavior is due to the contact graph becoming sparse when we use a small sample of the population. As building a sample of contact network happens to be an active area of research, we leave sampling out of the scope of this work [5]. We carried out our calibration on full contact network using the entire population for both cities.

We also observed that the R_0 is not stable when using small number of initial infections(I_0). The variation in R_0 decreases as we increase I_0. This behavior is shown in Figure 7 using three sample sizes of the population. We observe that as the population size increases, a higher value of I_0 is required to achieve a stable R_0. During calibration, we used $I_0 = 1000$ and while simulating the epidemic for 270 days, we started with an $I_0 = 200$.

5 Performance

klab The prototyping for this study was implemented in Python. The experiments were performed an Ubuntu machine each core having a speed of around 1 GiB. In this section, we comment on the run times for the *Auto Innovative* city. The run time of the entire script can be divided into four parts. First, the pre-processing of the output files from the transport simulator (SimMobility in this case). This part takes around 5 minutes to complete. Second, the creation of three sets of contact graph; Home graph, Activity graph and Transit Graph. Each set of graphs has 288 graphs- one for each 5 minute time of the day. The creation of graphs takes around 90 minutes for a full population of 4.5 million agents in the case of *Auto Innovative*. Third, the Union operation to combine each type of individual contact graph (*Home*, *Activity* and *Transit*) takes around 10 minutes using 10 threads in parallel. Fourth, the actual simulation for a period of 270 days takes around 9 hours.

There are several avenues where the performance can be improved. First, we can parallelise the graph creation process in temporal dimension. The contact graphs at different times of the day can be generated in parallel. Second, we can parallelise the actual simulation process, with each thread processing one component of the contact graph as shown in Figure 6b.

6 Pseudocode

Data Structure representing a contact Graph at timestep t ($G[t]$)

At every time-step t, the contact graph $G[t]$ is a set of two maps: {*forwardDicts*, *backwardDicts*}

forwardDicts is a Map $\langle$ key: $person_i$, value: $dummy_j\rangle$ `// representing an individual (`$person_i$`) who is present at a dummy location (`$dummy_j$`) at time` t

backwardDicts is a Map $\langle$ key: $dummy_j$,value: $[pid_1, pid_2, .., pid_{n_j}]\rangle$ `// where` n_j `is number of individuals at the location` $dummy_j$ `at time` t

PanCitySim Framework

$stateVector \leftarrow (S/E/I^A/I^S/R/D)$ for every person
Initialise $stateVector[person] = S \ \forall$ persons
$I_0 \leftarrow 200$
$\rho_{binary} \leftarrow$ use ρ from table to mark every person for a possible transition to I^S;

$day \leftarrow 1$ `// 270 days=9 months`
while $day \leq 270$ **do**
  $timestep \leftarrow 1$ `// we use 5-minute timesteps, total of 24*12=288 timesteps in a day`
  while $time - step \leq 288$ **do**
    $G \leftarrow G_{UNION[timestep]}$
    for *each dummy in* G **do**
      for *each person in* $G[backwardDict[dummy]]$ **do**
        if $stateVector[person] = I^A$ **then**
          $countInfect \leftarrow countInfect + 1$
      if $dummy = activity(W/E/S/O)\ node$ **then**
        $area \leftarrow (vornoi\ area\ of\ node(A_v))$
        $sample_{locs} \leftarrow$ ($countInfect$ locations in a circle using a Gaussian with $\sigma_x = \sigma_y = 0.0572 * A_v$)
        $reference_{loc} \leftarrow$ (1 location in a circle using a Gaussian with $\sigma_x = \sigma_y = 0.0572 * A_v$
        $mean_{dist} \leftarrow$(mean Euclidean distance between $reference_{loc}$ and $sample_{locs}$)
      if $dummy = Train$ **then**
        $mean_{dist} \leftarrow (A_{metro\ coach} * 0.2)^{0.5} * 0.5$
        $countInfect \leftarrow countInfect * \frac{1}{25}$
      if $dummy = Bus$ **then**
        $mean_{dist} \leftarrow (A_{Bus} * 0.25)^{0.5} * 0.5$
        $countInfect \leftarrow countInfect * \frac{1}{4}$
      if $dummy = Home$ **then**
        $mean_{dist} \leftarrow 6.5$
      if $countInfect > 0$ **then**
        for *each person in* $G[backwardDict[dummy]]$ **do**
          $\phi_{nt} = 1 - \exp\left(-\Theta'_{calibrated} * \frac{1}{mean_{dist}^3} * countInfect\right)$
          if $stateVector[person] = S$ **then**
            if $RAND(0,1) < \phi_{nt}$ **then**
              $stateVector[person] = E$
  for *each person in* $stateVector$ **do**
    use γ for transitions $I^S \rightarrow R$ *and* $I^A \rightarrow R$
    use age-specific μ for transitions $I^S \rightarrow D$
    use predetermined ρ_{binary} to choose $E \rightarrow I_A$ or $E \rightarrow I_S$
    use κ to realise the transition acoording to the path chosen in previous step

References

[1] K. Prem, Y. Liu, T. W. Russell, A. J. Kucharski, R. M. Eggo, N. Davies, S. Flasche, S. Clifford, C. A. B. Pearson, J. D. Munday, S. Abbott, H. Gibbs, A. Rosello, B. J. Quilty, T. Jombart, F. Sun, C. Diamond, A. Gimma, K. van Zandvoort, S. Funk, C. I. Jarvis, W. J. Edmunds, N. I. Bosse, J. Hellewell, M. Jit, and P. Klepac, "The effect of control strategies to reduce social mixing on outcomes of the COVID-19 epidemic in Wuhan, China: A modelling study," *The Lancet Public Health*, vol. 0, Mar. 2020.

[2] R. Verity, L. C. Okell, I. Dorigatti, P. Winskill, C. Whittaker, N. Imai, G. Cuomo-Dannenburg, H. Thompson, P. G. T. Walker, H. Fu, A. Dighe, J. T. Griffin, M. Baguelin, S. Bhatia, A. Boonyasiri, A. Cori, Z. Cucunubá, R. FitzJohn, K. Gaythorpe, W. Green, A. Hamlet, W. Hinsley, D. Laydon, G. Nedjati-Gilani, S. Riley, S. van Elsland, E. Volz, H. Wang, Y. Wang, X. Xi, C. A. Donnelly, A. C. Ghani, and N. M. Ferguson, "Estimates of the severity of coronavirus disease 2019: A model-based analysis," *The Lancet Infectious Diseases*, vol. 0, Mar. 2020.

[3] J. E. Cohen and D. Courgeau, "Modeling distances between humans using Taylor's law and geometric probability," *Mathematical Population Studies*, vol. 24, pp. 197–218, Oct. 2017.

[4] M. C. D. US Census Bureau, "Characteristics of New Housing." https://www.census.gov/construction/chars/highlights.html.

[5] M. Génois, C. L. Vestergaard, C. Cattuto, and A. Barrat, "Compensating for population sampling in simulations of epidemic spread on temporal contact networks," *Nature Communications*, vol. 6, p. 8860, Nov. 2015.